Ocean Engineering 312 (2024) 119191

Contents lists available at ScienceDirect

Ocean Engineering

journal homepage: www.elsevier.com/locate/oceaneng

Research paper

Accounting for power take-off efficiency in optimal velocity tracking control of wave energy converters

Adam Stock

Institute of Mechanical, Process and Energy Engineering, JN1.23, James Nasmyth Building, Heriot-Watt University, Edinburgh, EH14 4AS, Scotland, UK

ARTICLE INFO

Keywords:
Wave energy
Control
Ocean energy

ABSTRACT

There has been much research into how Wave Energy Converters (WECs) can capture energy from the waves and convert it into kinetic energy in the mechanical system (mechanical energy). However, because WECs typically generate power at high force and with low speed, the conversion of the mechanical energy into electrical energy can be inefficient. If Power Take-Off (PTO) efficiency is not accounted for in controller design then the efficiency of the WEC from wave energy to electrical energy can be poor. In this work, an adaptation of Optimal Velocity Tracking (OVT) control is presented, termed OVT-E, that accounts for PTO efficiencies in the controller formulation such that it converts more energy from the waves to electricity than traditional OVT approaches, termed OVT-M. Results show that, for an example WEC and PTO system in a simulation environment, OVT-E produces more efficient electrical energy conversion than OVT-M with lower forces through the drive-train. OVT-E is also shown to convert more electrical energy than an adaptive linear damping method. The methodology for designing OVT-E could have further applications when coupled with other controller implementations or if used alongside machine-learning for control co-design purposes.

1. Introduction

As the levelised cost of energy (LCOE) of wind and solar power continue to fall, wave energy is placed at a critical juncture in its development. Wave energy has potential for reducing both the magnitude and the degree of volatility in balancing requirements within future, wind and solar dominated power systems (Pennock et al., 2022a). However, wave energy is likely to only be successful as a major electricity source if it can reduce its LCOE, with a target of £90/MWh by 2035 (Pennock et al., 2022b).

The problem of maximising energy capture for narrow-banded wave energy converters (WECs) such as point absorbers has been explored thoroughly in the literature (notably in Falnes and Kurniawan (2020) for example), such that it is well known that an impedance matching controller is optimal for energy capture from the waves. The control problem is, however, acausal,[1] and so some form of approximation is required to implement these methods. A variety of approaches have been explored in the literature, (see, for example, Hals et al., 2011 for a range of typical approaches). Optimal Velocity Tracking (OVT) is one method explored in the literature (see Fusco and Ringwood, 2012 and García-Violini et al., 2020 for commonly used implementations), which has the advantage of simplicity of the controller and robustness of the control approach. The OVT method has since been used for two-body devices and for multiple degree of freedom devices (Stock and Gonzalez, 2020; Stock et al., 2018; Hillis et al., 2020). However, in all OVT methods in the literature, maximisation of the kinetic (or mechanical) energy capture of the WEC (perhaps within some limits) has been the goal.

When considering just the prime mover of a WEC system, it is sensible to design a controller that maximises the mechanical energy captured from the waves. When considering a WEC system as a whole, including a power take off (PTO) that includes losses (which may be variable and non-linear), the control problem is different, and the goal is to convert the maximum amount of energy from the waves into electrical energy output. Because the efficiency of the PTO often varies depending upon the required output, it is not necessarily the case that using the WEC prime mover to maximise mechanical energy capture from the waves results in the maximum electrical energy output. Hence, the controller must be designed differently.

PTO efficiency losses can be very large if the WEC, the controller and the PTO are poorly matched and may still be significant even if the PTO and WEC are matched relatively well (Ahamed et al., 2020; Penalba and Ringwood, 2019). For a given choice of WEC and PTO, it is therefore essential that the controller is designed with the efficiencies of the PTO in mind. In other words, the goal is to maximise the energy

E-mail address: a.stock@hw.ac.uk.

[1] Whilst commonly stated and indeed true from the perspective of wave height to control action, it should be noted that, as with all real dynamics, the problem is not truly acausal if viewed from an alternative perspective (see Coe et al., 2021 for a discussion on this point).

https://doi.org/10.1016/j.oceaneng.2024.119191
Received 17 July 2024; Received in revised form 23 August 2024; Accepted 3 September 2024
Available online 12 September 2024

converted from energy in the waves to electrical output accounting for the WEC and PTO system as a whole.

The issue of maximising converted electrical energy from the waves has begun to be considered by some researchers outwith OVT control. In Coe et al. (2021), an equivalent impedance of the whole system is considered by using the Thévenin equivalent circuit of an electrical PTO. Such an approach is useful but requires in depth knowledge of the PTO design (beyond a simple efficiency map) and assumes that the PTO is an electrical circuit suitable for Thévenin equivalence. In Bacelli et al. (2015), a controller is designed for a flap device that accounts for viscous drag and PTO efficiencies. The work is less a practical implementation for a controller and more focused on the implications of PTO efficiency and viscous drag effects through mathematical modelling of the particular flap device system under monochromatic waves.

In addition to sub-optimal electrical energy conversion, if the components of a WEC system are considered separately, and so the mechanical energy capture of the WEC is optimised, large mechanical forces are often required from the PTO — particularly when a WEC is operating off-resonance, as the mechanical reactive power demands can be very large. These large forces, typically at low speeds, often lead to inefficient conversion to electrical energy whilst simultaneously inducing large loads on WEC components.

When considering the design of a WEC system (WEC prime mover, PTO and controller), the LCOE is a function of the energy capture and capital expenditure (CAPEX), and the operational expenditure (OPEX). More specifically, LCOE is calculated as,

$$LCOE = \frac{\sum \frac{I_t+M_t+F_t}{(1+r)^t}}{\sum \frac{E_t}{(1+r)^t}} \tag{1}$$

where, I_t is the initial cost of investment expenditures, M_t is the Operations and Maintenance (O&M) costs, F_t is the fuel expenditures (typically zero for renewables), with E_t the sum of all electricity generated, t is time and r the discount rate. Increasing the amount of electricity generated lowers LCOE, whilst decreasing CAPEX and/or OPEX achieves the same aim. It is useful to note that the electrical energy generated is a function of the availability of the device as well as its efficiency. Availability is often, in turn, a function of the loads on the system (higher loads lead to more component failures and more downtime and/or narrower operational limits).

Hence, in the author's opinion, controller designs that consider the control of the WEC separately from the PTO, and so focus on maximising mechanical energy capture, might not be the best option for minimising LCOE of electricity producing WEC systems. Such designs may have high loads that could require larger, more costly components and potentially increase the number of failures, increasing O&M costs and reducing availability.

Cognisant of these factors, implementing an OVT methodology that maximises electrical energy capture for a WEC system including the PTO may decrease LCOE by increasing electrical energy conversion and reduce O&M costs through reduced mechanical forces. The design, tuning, implementation and software testing of a novel implementation of OVT control that aims to maximise electrical energy output, rather than mechanical energy capture, is the focus of the work presented here. The objective of the work is to describe and implement a new methodology for designing OVT controllers in a simulation environment to demonstrate improved electrical energy capture compared to previous OVT implementations.

In Section 2, the theoretical methodology for design and tuning of a novel OVT approach for maximising electrical energy conversion accounting for power take-off efficiency is described. In Section 3, the implementation of the methodology is discussed and presented. Simulations, using both regular and irregular waves, are run and the results are presented in Section 4. In Section 5, the results are discussed, including implications for the design of wave energy converter controllers in the future, with conclusions presented in Section 6.

2. Methodology

In this section, the methodology used to design an OVT controller that accounts for PTO efficiency is described.

2.1. Optimal velocity tracking overview

It is first necessary to describe the formulation of a 'typical' OVT controller that aims to maximise the conversion of energy in the waves to mechanical power. The familiar result of maximum mechanical energy capture through impedance matching can be derived,[2] a version of which describes the optimal velocity for maximising mechanical energy capture from the waves in the frequency domain as,

$$v(\omega) = \frac{F_E(\omega)}{2B(\omega)} \tag{2}$$

where v is the optimal velocity, F_E is the excitation force, and B is the radiation resistance of the WEC. Typically, OVT control finds the optimal velocity v for the excitation force frequency ω and sets it as a reference velocity that is tracked by a disturbance rejection controller.

Using an estimate of the excitation force, $\hat{F}_{exc}$, and an estimate of the dominant excitation force frequency, $\hat{\omega}$, a basic OVT-M structure is as shown in Fig. 1, where $H(\hat{\omega})$ is a real time estimate of $2(B(\hat{\omega}))$ based on the estimated excitation force frequency, and $C(s)$ is a reference tracking controller.

Clearly, some form of estimate of excitation force, $\hat{F}_{exc}$ and dominant excitation force frequency $\hat{\omega}$ must be provided. One method is to use an inverse model of the WEC dynamics and an Extended Kalman Filter (Stock et al., 2019, 2018, 2020). Applying this method gives the control structure shown in Fig. 2, referred to in this paper as OVT-M.

2.2. Optimal velocity tracking for electrical energy conversion

In the case of a WEC designed to produce electrical power, the goal is not necessarily to capture the maximum amount of energy from the waves. Instead, the goal is to convert the maximum amount of energy from the waves into electricity. This subtle difference requires the controller to account for the efficiency of the power take-off (PTO).

Considering the regular wave case, the WEC intrinsic mechanical admittance (the inverse of the intrinsic mechanical impedance) is represented by $Y = \frac{1}{Z}$, which, for regular excitation force with frequency ω, can be represented by a complex number $A_Y e^{j\phi_Y}$, where the amplitude A_Y and phase ϕ_Y are functions of ω. Defining the input excitation force in the time domain as $F_E = A_E e^{j(\omega t)}$, and the PTO force $F_P = A_P e^{j(\omega t+\phi_P)}$ (with all amplitudes and phases functions of the frequency ω), the resultant WEC velocity, V, is given by,

$$A_V e^{j(\omega t+\phi_V)} = (A_E e^{j(\omega t)} + A_P e^{j(\omega t+\phi_P)})A_Y e^{j\phi_Y} \tag{3}$$

The efficiency profile of a PTO can be highly non-linear and so solving the analytical equations is not easily achievable. Nonetheless, over one period, T, the electrical energy captured is given by,

$$E_{elec} = \int_0^T \eta(\cdot,t)(-F_P(t)V(t))dt \tag{4}$$

where η is the efficiency that could be a non-linear function. Efficiency may be a function of a wide variety of variables, however it is commonly a non-linear function of the velocity, the PTO force, or both.

Using Eqs. (3) and (4), the amplitude, A_P, and phase, ϕ_P, of the PTO force F_P that maximises the electrical energy capture can hence be found for a range of excitation force frequencies, as well as the amplitude A_V and phase ϕ_V of the resulting velocity.

[2] Proofs are readily available in the literature, notably in Falnes and Kurniawan (2020).

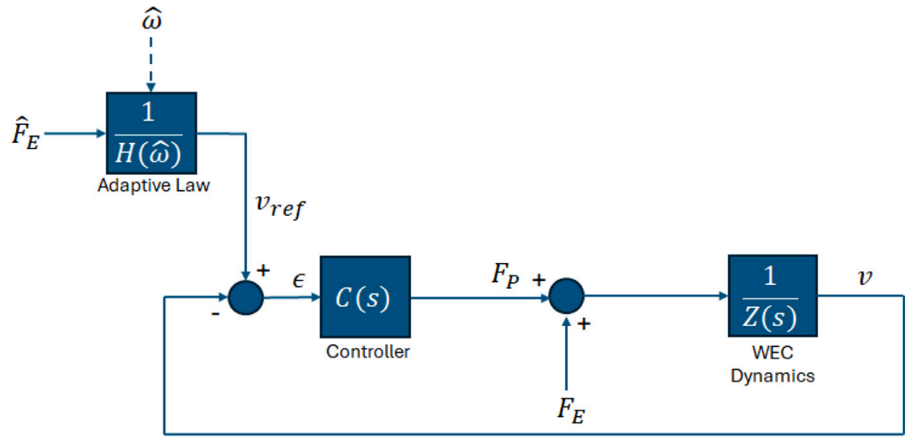

Fig. 1. Basic Optimal Velocity Tracking Structure. Note the dashed line indicates that the value is used to schedule the gain.

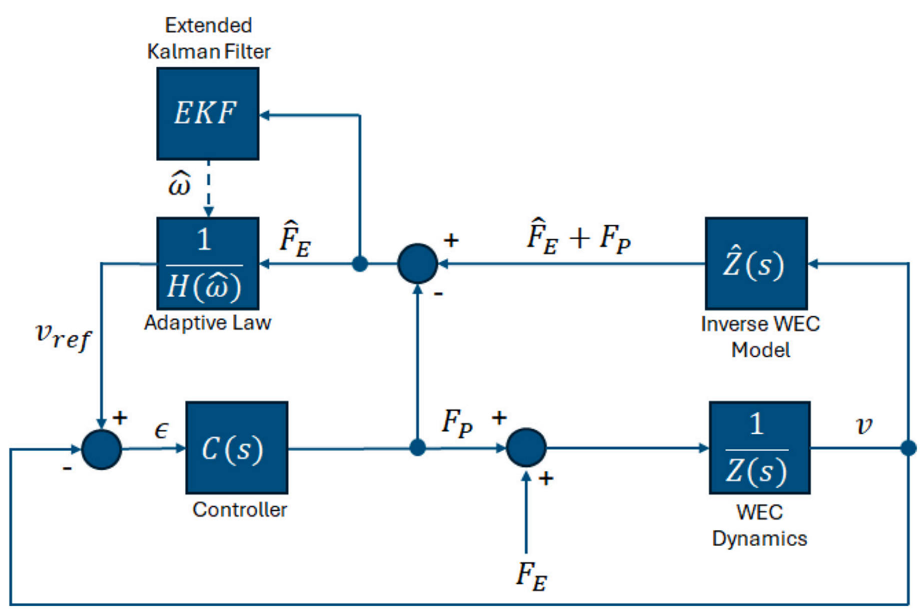

Fig. 2. An Optimal Velocity Tracking implementation for mechanical power capture using an inverse model and an extended Kalman filter. Note the dashed line indicates that the value is used to schedule the gain (OVT-M).

Hence, using the optimal values of $A_P(\omega)$, $\phi_P(\omega)$, $A_V(\omega)$, and $\phi_V(\omega)$ for a range of values of ω that cover the operational range of the WEC, an adapted model M_V can be found by,

$$\frac{1}{M_v(\omega)} = H(\omega) + \frac{A_P(\omega)}{A_V(\omega)} e^{(j(\phi_P(\omega)-\phi_V(\omega)))} \tag{5}$$

The magnitude and phase of $\frac{1}{M_V}$ is plotted across a range of frequencies to create a ‘pseudo-Bode’ plot, i.e. a plot of gain and phase of the non-linear function using the same format as a Bode plot of a linear function. A transfer function, $M_e(s)$ that approximates the ‘pseudo-Bode’ plot is then fitted.

An adapted controller structure, called OVT-E, is shown in Fig. 3. The OVT-M structure from Fig. 2 has been adapted by replacing the inverse WEC model with an adapted inverse WEC model for calculation of the input to the adaptive law. Assuming a suitable model $M_e(s)$ can be found and implemented, the controller should track a reference speed that is optimal for electrical energy conversion. If the range of PTO forces used in deriving the model is limited to the maximum output of the PTO and if results where the velocity exceeds the PTO limits are excluded in the derivation, then the controller will typically operate within these limits.

2.3. Stability

The model can be redrawn to consider the stability of the system from the input of excitation force, F_E to the output of power take-off force, F_P, as shown in Fig. 4.

Fig. 4 shows that the system has a unity feedback loop with a positive sign on the comparator. Hence, the system stability can be ascertained by considering the open loop system,

$$G_{OL} = \frac{C(s)}{H(\omega)} + \frac{C(s)}{Z(s)} - \frac{M_e(s)C(s)}{Z(s)H(\omega)} \tag{6}$$

Eq. (6) assumes that a Laplace representation of the impedance is a reasonable approximation of the WEC. Note that, for an excitation force dominant frequency of interest, the scheduled variable $H(\omega)$ is constant across the frequency range.

3. Implementation

In this section, the challenges and adaptations required for implementing the OVT-E methodology are discussed using an example WEC and PTO combination.

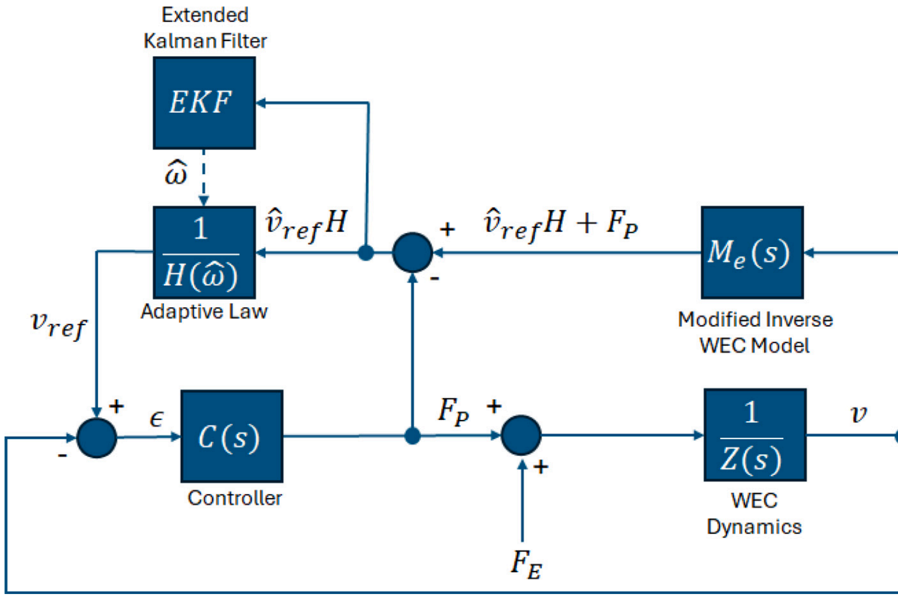

Fig. 3. An adapted Optimal Velocity Tracking implementation using an adapted model. Note the dashed line indicates that the value is used to schedule the gain.

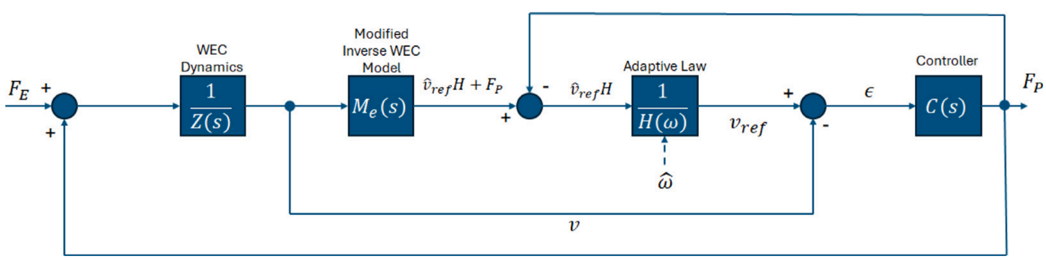

Fig. 4. Rearranged OVT-E controller considering stability.

3.1. Application of OVT-E

To help discussion of the implementation of the OVT-E approach, an example WEC and PTO are used. The WEC used is 'WEC-2', a submerged single body point absorber with a 20 m diameter and 5 m height (Stock et al., 2019), the NEMOH mesh of which is shown in Fig. 5 for illustrative purposes. There is 5 m distance from the top of the WEC prime mover to the mean water level. The PTO model used is the efficiency curves for the Trident 'Power-Pod', a PTO originally designed for use with linear damping methods. To provide the required power to match to the WEC, 18 sets of 6 Trident LGF30 PTOs were used, a linear generator PTO. These allow a peak force of 3.24 MN, with a maximum stroke of 10 m and a maximum allowable velocity of ±2 m/s (Trident Energy, 2014). Illustrative diagrams of the Trident PTO are shown in Fig. 6, and the efficiency curves for each LGF30 PTO are shown in Fig. 7. Note that neither the WEC nor the PTO are designed with a view of being an optimal pairing, or even being particularly well suited to OVT. Instead they are chosen as representative of technology that could be used and to highlight the challenges of PTO efficiency, control for electrical power output and co-design. Using Eqs. (3) and (4), with a model of the WEC created using the Cummins' equation method as described in Stock and Gonzalez (2020), the optimal PTO force and corresponding velocity profile for maximum electrical energy conversion is found for a range of excitation force frequencies. The range of PTO forces used in the derivation is limited to those that are within the limits of the PTO. Any results where the velocity exceeds the velocity limit of the PTO are excluded. Hence, using Eq. (5), the model $M_v(\omega)$ is derived as a set of phases and magnitudes for a range of excitation force amplitudes. The inverse of $M_v(\omega)$ (for excitation forces of amplitude 2MN) is plotted using crosses in Fig. 8, alongside the

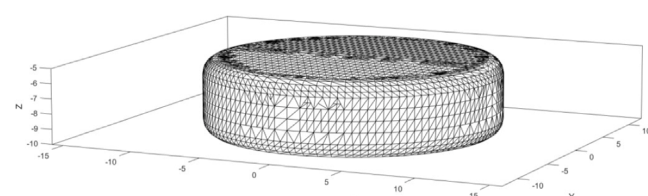

Fig. 5. Hydrodynamic mesh of 'WEC-2' used in NEMOH for hydrodynamic modelling (approx. 1600 panels).

admittance of the WEC, $\frac{1}{Z(\omega)}$, which is plotted with circles. Transfer function approximations of both are created using the methodology in Valério et al. (2008) and are also shown in Fig. 8 as dashed lines. Whilst the approximation $\frac{1}{Z(s)}$ is reasonably accurate across the range of frequencies of interest, the phase approximation of $\frac{1}{M_e(s)}$ is not accurate. The phase is critically important in impedance matching control and so a manual fitting approach that focuses exclusively on the appropriate phase of the transfer function approximation is used.

Hence, a transfer function, $\frac{1}{M(s)}$ is designed that matches the phase of $\frac{1}{M_v(\omega)}$ well. A third order approximation is used that matches the phase well across the main frequencies of operation. The model is designed as,

$$\frac{1}{M(s)} = (1 \times 10^{-6})\frac{s^2 + 0.27s + 0.7}{s(s+1.6)(s+1.1)} \tag{7}$$

and is shown plotted alongside $\frac{1}{M_v(\omega)}$ in Fig. 9. As the derivation of the optimal model $M_v(\omega)$ includes limits on excitation force and WEC

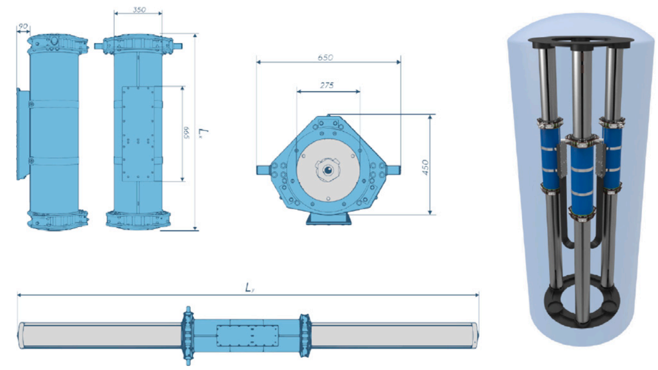

Fig. 6. Schematics of Trident PTOs for illustrative purposes (from Trident Energy, 2014).

velocity, the optimal model is slightly different for different excitation force amplitudes. As, for the implementation presented here, the difference is not large for the main frequencies of operation, the model based on an excitation force amplitude of $2MN$ is used.

As $M_e(s)$ was fitted to match the phase well, the gain must be adjusted through a gain that is scheduled on an estimate of the excitation force frequency, $k(\hat{\omega})$. For the regular wave case, gain scheduling in this way ensures that the gain scheduled model is very well matched. Assuming a narrow-banded excitation force spectrum, the model will also be well matched for irregular waves.

The potential implementation of the OVT-E controller shown in Fig. 3 could be used (with adaptation to account for gain scheduling), in which the inverse WEC model $M_v(s)$ (or, the gain scheduled model $k(\omega)M(s)$) is directly fed the WEC velocity v. This implementation is possible even if the model M_v is improper by one order of s by using the methodology previously used to implement the excitation force estimator in Stock et al. (2019). However, a different implementation is used here, as shown in Fig. 10.

The alternative implementation has two key advantages over that of Fig. 3. Firstly, the transfer function $\frac{M(s)}{Z(s)}$ is not improper, making implementation simpler. Secondly, the implementation caters for other excitation force estimators to be used in place of the inverse WEC model $\hat{Z}(s)$ implemented here, making the implementation more adaptable.

3.2. Extended Kalman filter

The OVT-E implementation requires a value of the dominant excitation frequency ω, provided here by an estimate, $\hat{\omega}$, from an extended Kalman filter (EKF) that is implemented as per (Stock et al., 2019). The EKF requires an estimate of the excitation force $\hat{F}_E$ as an input, which is calculated using the Laplace domain estimation model $\hat{Z}(s)$ detailed in Section 2 as per the method in Stock et al. (2019) and Stock and Gonzalez (2020).

For submerged WECs, it is suggested (Sergiienko et al., 2017, 2019) that the EKF may estimate the frequency of the excitation force with some bias, owing to the band pass properties of submerged WECs. In the case of the WEC used in this work, the excitation force has a fairly broad bandwidth, with the EKF estimating a sensible value for the peak frequency. Examples are shown in Fig. 11.

3.3. Stability

The stability of the OVT-E controller can be checked using Eq. (6), adjusted to include the scheduled gain $k(\hat{\omega})$, and necessarily linearised at the scheduling frequency $\hat{\omega}$,

$$G_{OL} = \frac{C(s)}{H(\hat{\omega})} + \frac{C(s)}{Z(s)} - \frac{M(s)k(\hat{\omega})C(s)}{Z(s)H(\hat{\omega})} \tag{8}$$

Table 1
Varying Gain to Ensure Stability.

Period	4	5	6	7	8	9	10	11	12	13	14	15
k_s	0.73	1	1	1	1	1	0.84	0.61	0.50	0.44	0.40	0.37

Particularly at higher wave periods (lower frequencies) the system is unstable. To ensure stability, the scheduling gain $k(\hat{\omega})$ can be adjusted by,

$$k(\hat{\omega}) = k_s(\hat{\omega})k_m(\hat{\omega}) \tag{9}$$

where $k_m(\hat{\omega})$ is the original gain scheduling and $k_s(\hat{\omega})$ is a number less than one that maintains stability of the controller, see, for example, the Nyquist plots for a period of 12 s with and without the adjustment to the gain k_s in Fig. 12.

Adjusting the gain in this manner necessarily makes the controller sub-optimal, as the optimal gain is that of $k_m(\hat{\omega})$, however, the controller must be stable to function correctly. The adjustment $k_s(\hat{\omega})$ for a range of periods for the example WEC and PTO combination used in this work is given in Table 1.

4. Results

To test the OVT-E controller, a WEC-Sim (Keester et al., 2022; Ogden et al., 2022) model of 'WEC-2' (Stock et al., 2019), and the efficiency curves for the Trident 'Power-Pod' PTO (Trident Energy, 2014) are used to model the WEC and PTO system. Note that the electrical dynamics of the PTO are not modelled directly, the efficiency curves are simply applied to the mechanical force and speed values from WEC-Sim to calculate the electrical power. For comparison to OVT-E, an OVT-M controller (aiming to maximise mechanical power) is designed as per (Stock et al., 2019) and a linear damping controller that adapts the gain based on an estimate of the frequency (referred to here as Adaptive Linear Damping or ALD) is also designed (Stock et al., 2019). Finally, the OVT-E controller described in the previous sections is implemented.

All the controllers have a hard limit set on the force demand at the maximum force of 3.24MN. The OVT-M controller also has position and acceleration constraints applied as per (Fusco and Ringwood, 2012; Stock et al., 2020).

A series of regular wave simulations are conducted across periods from 5 s to 14 s, and wave heights 1 m to 4 m using each of the three controllers. Next, a set of Pierson–Moskovitch spectrum irregular wave simulations are conducted across the same wave period and wave height ranges, with each wave height and period combination given a unique seed for random generation of the waves. All simulations have transients of the simulation and controller start up removed, leaving 500 s of simulation data. In each case, the mean electrical power, the mean mechanical power and the PTO force demands are assessed.

4.1. Regular wave simulations

Regular waves do not occur at sea, however, they are a useful way of confirming that the controller is stable and of demonstrating the improved electrical energy conversion compared to other methods. Fig. 13 shows the mean power in MW of the WEC, controlled using OVT-E, ALD and OVT-M for regular waves of varying wave height and wave period.

OVT-E and ALD always produce positive electrical power, and OVT-E consistently produces more power than ALD, though the difference is small at higher periods where, to maintain stability, the gain of the OVT-E controller has been constrained. OVT-M often produces negative electrical power, which may initially be a counter-intuitive result. However, the negative power is purely a result of generating and consuming power at low efficiencies. When the mechanical power

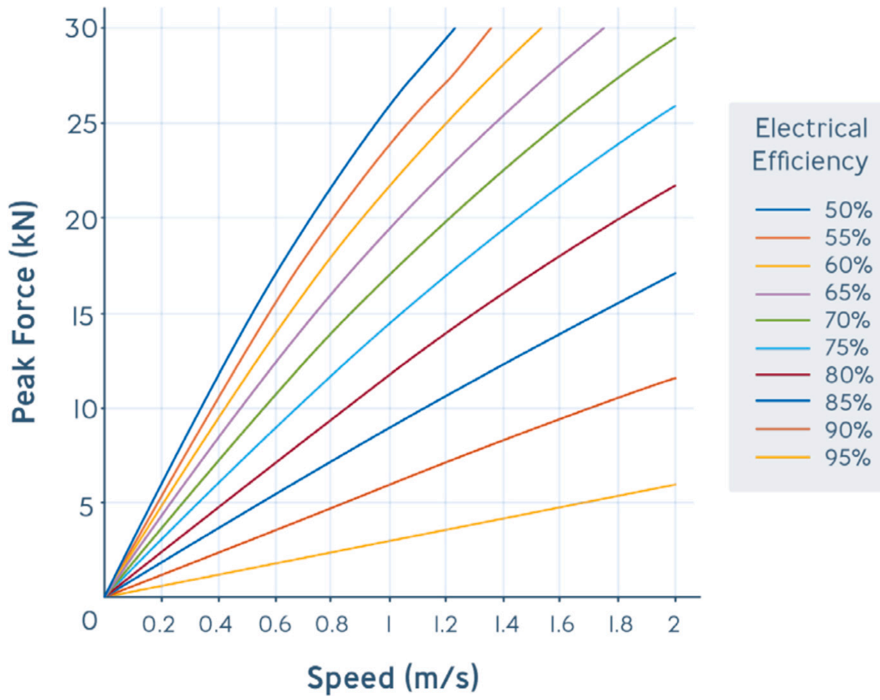

Fig. 7. PTO efficiency map between PTO force and speed for Trident Power-pod PTO.

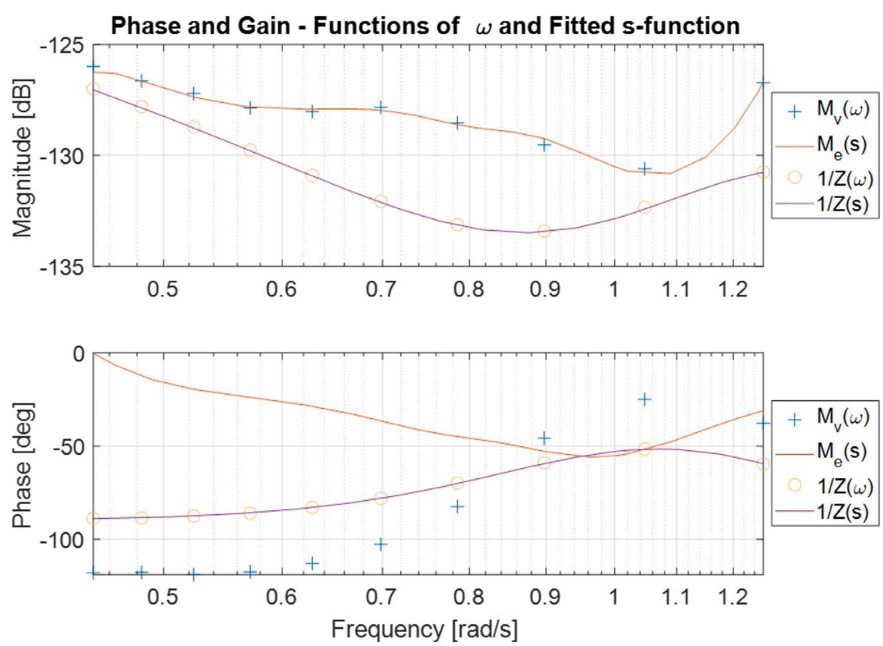

Fig. 8. Magnitude and phase of $M_v(\omega)$, $M_e(s)$, $\frac{1}{Z(\omega)}$ and $\frac{1}{Z}(s)$.

capture is considered, Fig. 14 shows that OVT-M is performing well via the metric to which it is designed. It is also notable that the mechanical power capture of OVT-E is, in most cases, significantly lower than OVT-M, and closer to the values of ALD. There are some cases where this is not true, for example periods of 8 s to 10 s in wave heights of 4 m. This is explained by the fact that OVT-M requires larger forces than can be provided at these periods to maximise the mechanical power capture and so the hard limits on force are being applied. A lower force at a different phase, such as that which happens to be provided in this case by OVT-E, can result in higher mechanical power capture.

The maximum force demand for each controller, across different wave heights and periods, is shown in Fig. 15. Force demand is a useful indicator of the potential capital and operational costs (CAPEX and OPEX), as higher forces are more likely to result in more expensive designs to withstand the force and/or more failures of components and hence more down-time for repair.

OVT-E has consistently lower force demand than OVT-M. Further, combining the maximum force plot in Fig. 15 with the time domain plots of force demand for some selected periods and frequencies in Fig. 16, it is shown that OVT-M consistently saturates the PTO at higher periods. OVT-E tends to keep within the limits of the PTO, and, in the most extreme conditions when PTO force is saturated with OVT-E (e.g. wave height 4 m, wave period 8 s), the demand beyond the limit is small compared to OVT-M. More typical operation (see

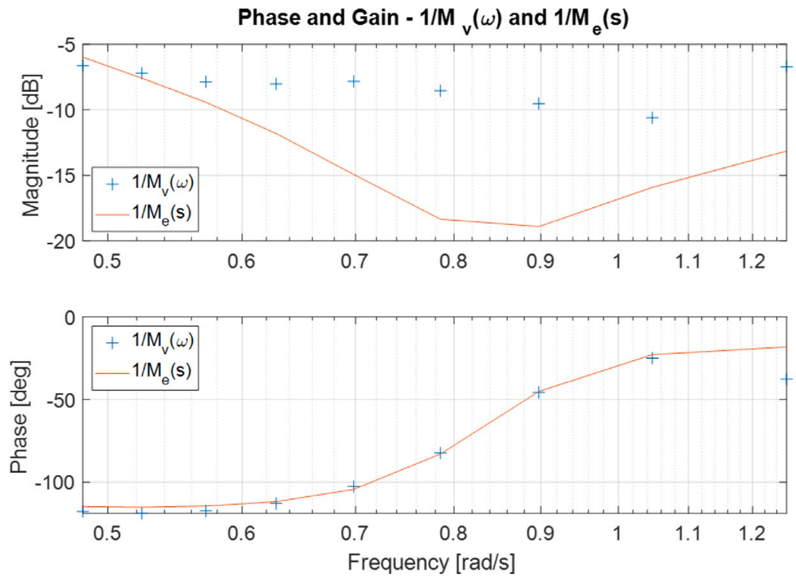

Fig. 9. Magnitude and phase of $M_v(\omega)$ and the manually fitted $M_e(s)$.

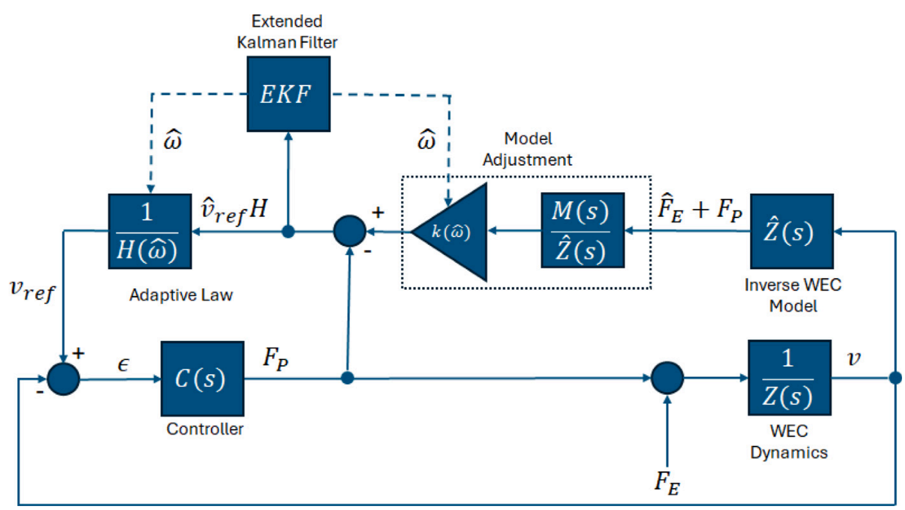

Fig. 10. The OVT-E controller rearranged for easier implementation.

Fig. 16, wave height 1 m, period 8 s) shows OVT-E with substantially lower force demand than OVT-M but slightly increased force demand compared to ALD. The exception is at higher wave periods, where ALD has both higher forces and either lower or approximately equal power capture compared to OVT-E. The better matched phase of OVT-E enables approximately equal electrical power capture at lower forces. A time-domain example of the force demand being higher for ALD than OVT-E can be seen in Fig. 16 with wave height 2 m, period 14 s.

4.2. Irregular wave simulations

The results for irregular wave simulations follow the same general pattern as the results for regular waves. Observing Fig. 17, OVT-E typically produces the largest amount of electrical power, ALD produces the second most and OVT-M produces the least. In some conditions, OVT-M produces negative electrical power, but, from Fig. 18 it is seen that OVT-M is typically the best performing controller for mechanical energy capture.

However, there are some exceptions to the typical results. For irregular wave heights of 1 m, OVT-E is outperformed in electrical power by ALD for periods of 13 s and 14 s. The exceptions are discussed further in Section 5.

The average power levels are low for the device size though at times the mechanical power output does reach the rated value with OVT-M, with a small number of occurrences at large wave heights. The velocity limiting method described in Fusco and Ringwood (2012) typically constrains the velocity well with only a few exceptions. For OVT-E, the mean velocity amplitude is much lower than that of OVT-M and the maximum velocity (2 m/s) is never exceeded (see Figs. 19 and 20). The mean force amplitude and the maximum force demand are also always equal or lower for OVT-E compared to OVT-M (see Figs. 22 and 23). It is worth reiterating that the PTO and WEC used here are not designed to be well matched and so the low electrical power output is not unexpected.

5. Discussion

In this section the results are discussed in three parts. Firstly, in Section 5.1 the common results that are typical across the operational envelope are discussed. Secondly, in Section 5.2, exceptions or non-typical results are discussed. Finally, in Section 5.3, some general remarks that expand on the results to discuss potential future work are presented.

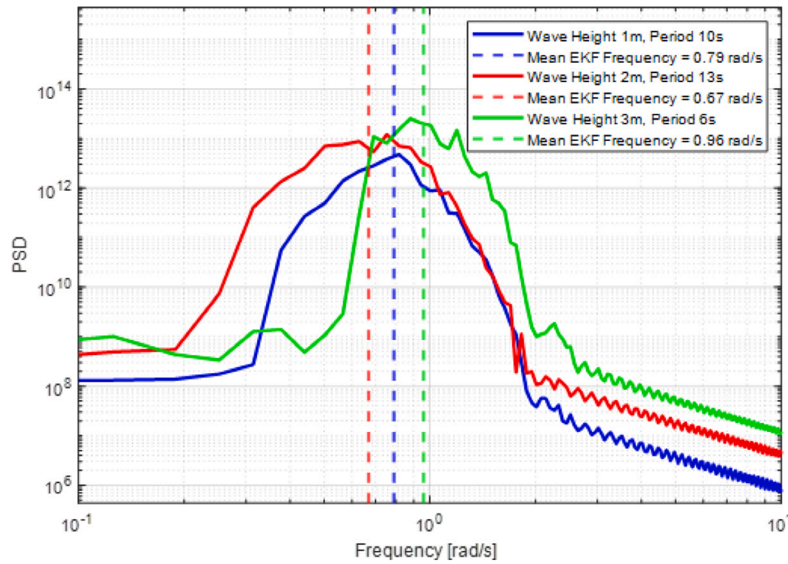

Fig. 11. Spectra of excitation force for three simulations with varying wave height and wave period. Dashed lines show the mean estimated excitation force frequency output from the EKF.

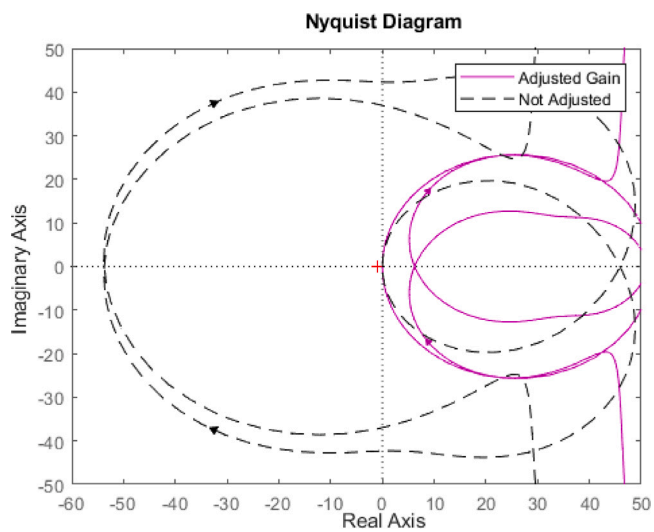

Fig. 12. Nyquist plot of the system G_{OL} at a period of 12 s with and without the adjusting gain k_s.

5.1. Typical results

Observing first the results for regular wave simulations, OVT-E outperforms OVT-M in electrical power conversion in all conditions, whilst also converting **less** power from the waves into mechanical energy. OVT-E also converts more electrical energy than the ALD controller and captures more mechanical power than ALD. These results are inline with expectation, as OVT-E provides some mechanical reactive power flow through the system, increasing mechanical power capture compared to ALD, but limits the mechanical reactive power flow through the system to avoid operating at highly inefficient operating points. Observation of the time domain plots in Figs. 16 and 21 show that OVT-E results in a different phase and gain of the PTO response, as expected.

OVT-E's lower mechanical energy conversion compared to OVT-M leads to lower mean force amplitude, which would be expected to reduce mechanical loads through the drive train, potentially lowering LCOE. In most conditions ALD has lower force demand than OVT-E, however this is accompanied by less electrical power conversion.

For irregular waves the same observations are true, except in the smallest waves at the highest wave period (see Section 5.2), demonstrating OVT-E could potentially be implemented on a real system - i.e. regular waves are not required for OVT-E to work well.

In all cases (both regular and irregular waves) OVT-E keeps the PTO velocity within the limits of the system (2 m/s). For OVT-M, whilst the velocity is typically kept within these limits there are some wave conditions in which the limits are exceeded. The reason for this difference between OVT-E and OVT-M is that whilst OVT-M has a soft limit on the PTO velocity the controller design does not inherently take into account PTO velocity limits. Because tunings of OVT-E in which velocity exceeds the limits are rejected during the controller tuning process, limits are an inherent part of the OVT-E implementation.

5.2. Exceptions

There are some exceptional cases where OVT-E is outperformed by ALD for irregular waves, specifically in waves of 1 m wave height and periods of 13 s and 14 s. A possible reason for the under performance is the reduced gain required to keep the system stable, with smaller wave heights more affected due to the generally less favourable efficiency conditions of lower PTO velocities.

With zero model mismatch (i.e. a perfect control design model) and perfect reference speed tracking, the PTO force for OVT-E would be kept within the set limits at all time. However, imperfections in model matching and imperfect reference speed tracking means that in some conditions the PTO force demand for OVT-E exceeds the maximum value and is limited by the hard limit (e.g. Fig. 16 for wave amplitude 4 m and period 8 s). Any exceedance of the maximum force for OVT-E is small compared to OVT-M. In some regular wave conditions OVT-E has a lower mean force amplitude than ALD, despite higher electrical power conversion (see Fig. 15, periods above 12 s) including some cases in which OVT-M exceeds the force limits (see Fig. 16, wave height 2 m, period 14 s).

5.3. Future work

The OVT-E methodology could be extended to other single body WECs and other PTO systems for which efficiency is a function of speed and/or force with minimal adaptation required. The designer does not need to know the details of the PTO design, they only require information on the efficiency that could be obtained easily via experiment. For

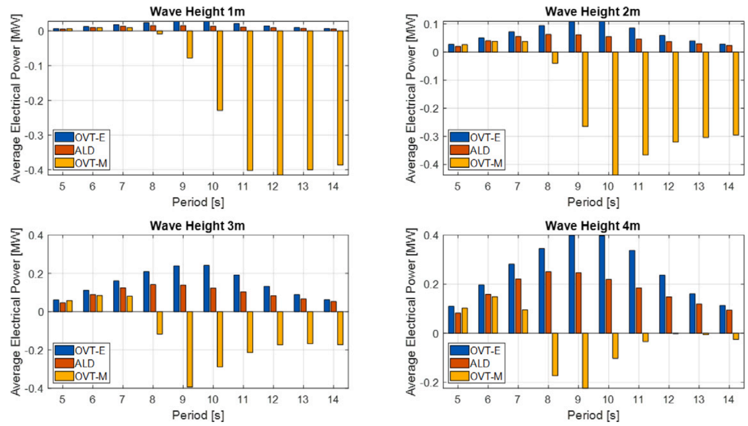

Fig. 13. Average Electrical Power — Regular Wave Simulations.

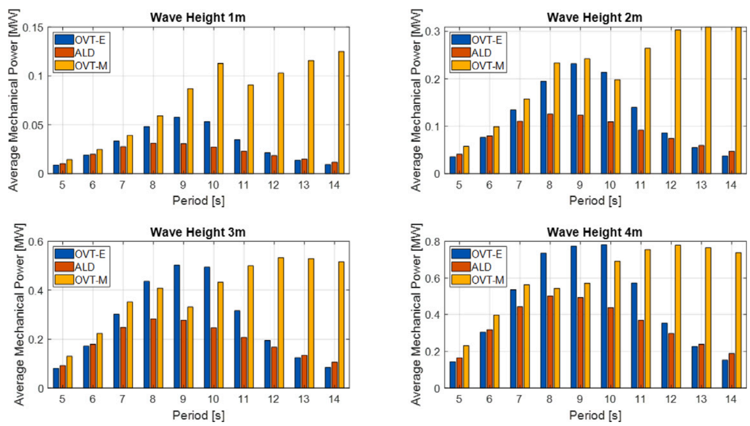

Fig. 14. Average Mechanical Power — Regular Wave Simulations.

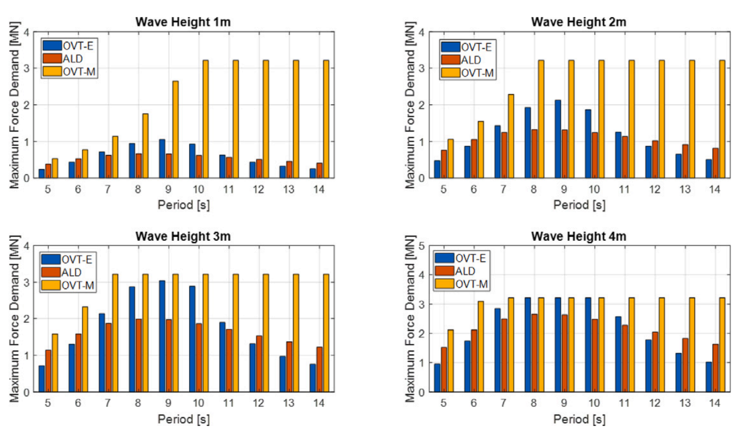

Fig. 15. Maximum Force — Regular Wave Simulations.

multi-body WECs, the OVT-E methodology could be applied with some adaptation of the mechanical impedance term to account for the more complex dynamics. PTOs for which efficiency is a function of other variables could also be incorporated into the methodology with some adaptation. Hence, OVT-E has the potential to be utilised on a broad range of wave energy systems.

The use of Eqs. (3) and (4), used to derive $M_v(\omega)$, which details the best phase and gain of the system for maximum electrical energy conversion, could be coupled with other control methods such as the PI control approach of Coe and Bacelli (Coe et al., 2021), to quickly and easily adapt the controller for PTO efficiencies without detailed knowledge of the PTO design.

If the design of the PTO is known and can be altered, then Eqs. (3) and (4) could be used to help co-design WEC-PTO-Controller systems through machine learning methods such as genetic algorithms. As the equations are simple regular time domain equations, they can be easily incorporated into machine learning methods.

Limitations on this work include the use of only a single example WEC and PTO and no accounting for more complex non-linearities of the WEC dynamics. Future work within the ongoing HAPiWEC project, of which this paper is an output, will address these issues through implementation of the controller in a wave tank environment for a scaled WEC and PTO system.

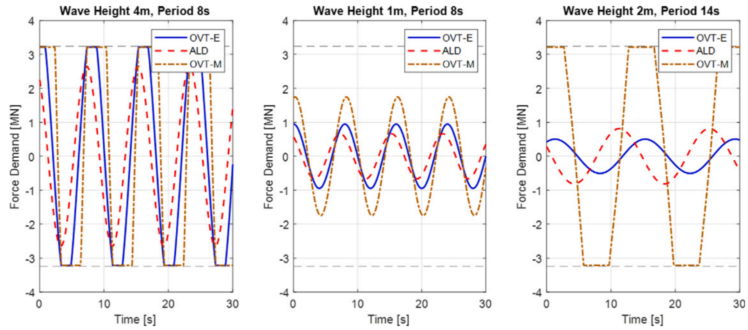

Fig. 16. PTO Force in the Time Domain — Regular Wave Simulations (Selected Examples).

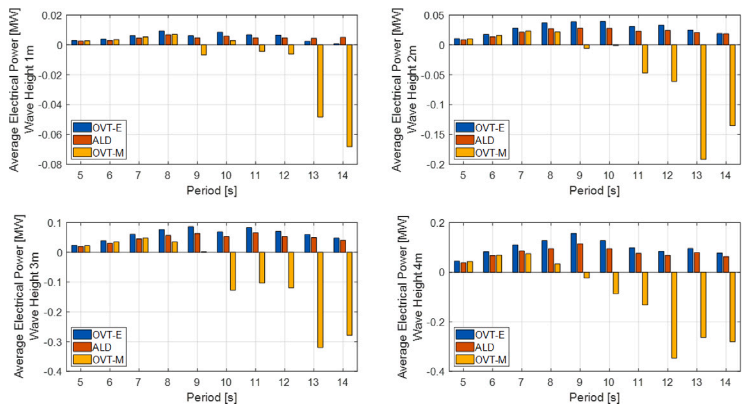

Fig. 17. Average Electrical Power — Irregular Wave Simulations.

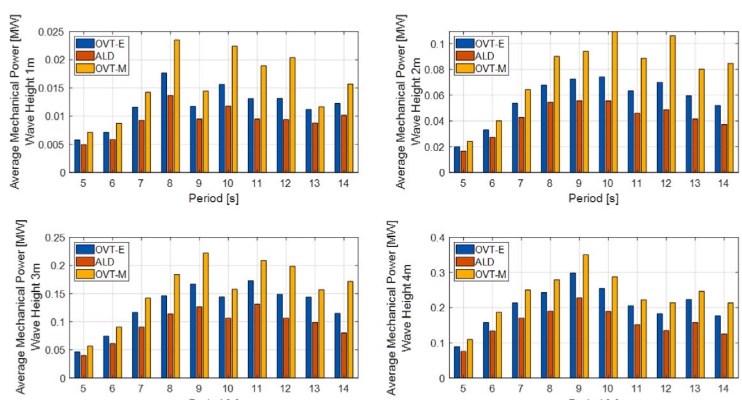

Fig. 18. Average Mechanical Power — Irregular Wave Simulations.

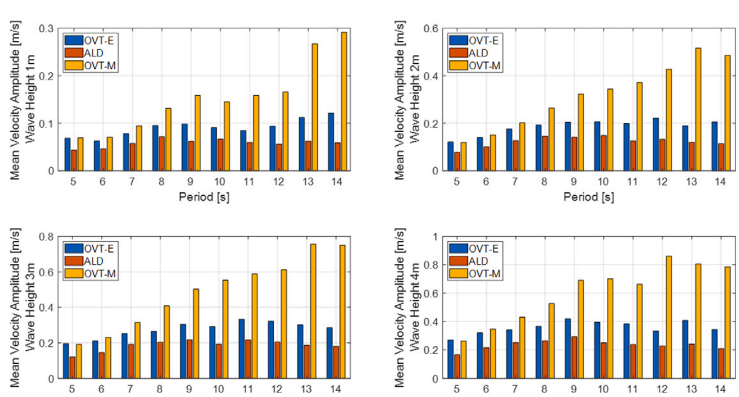

Fig. 19. Mean PTO Velocity Amplitude — Irregular Wave Simulations.

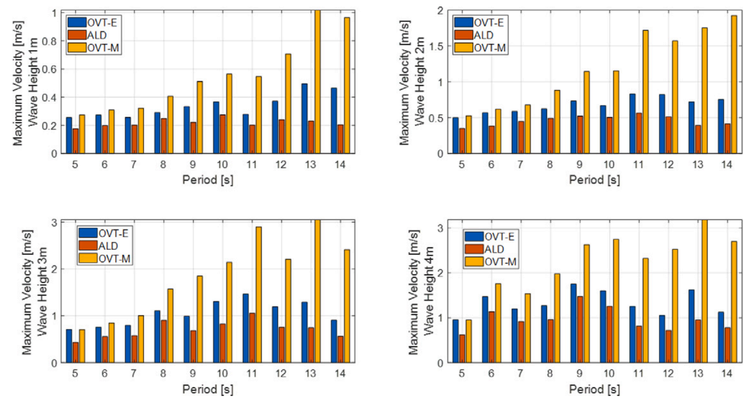

Fig. 20. Maximum PTO Velocity — Irregular Wave Simulations.

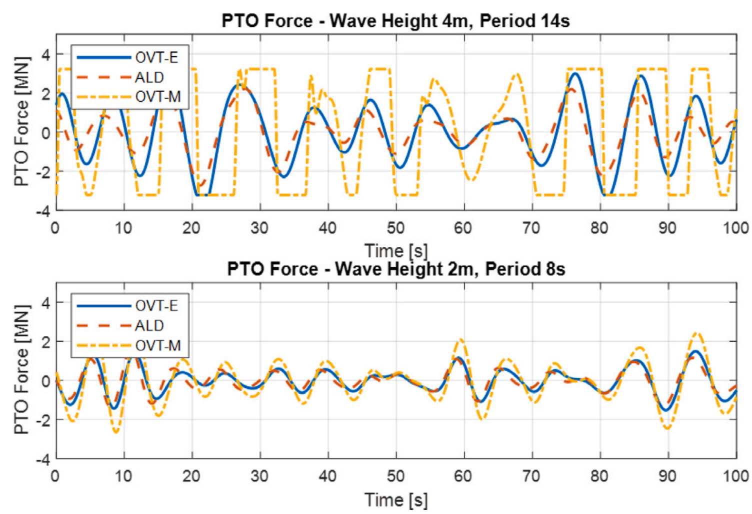

Fig. 21. PTO Force in the Time Domain — Irregular Wave Simulations (Selected Examples).

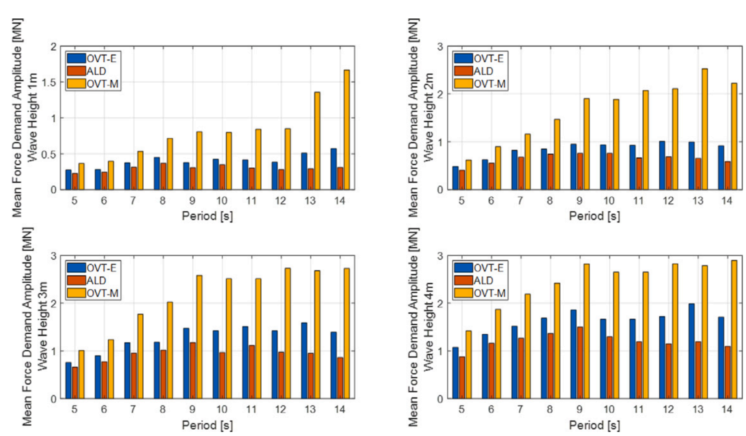

Fig. 22. Mean PTO Force Amplitude — Irregular Wave Simulations (Selected Examples).

6. Conclusions

In this work, an adaptation to Optimal Velocity Tracking (OVT) control has been detailed, whereby the controller is designed to maximise electrical energy conversion rather than mechanical energy capture, requiring no more detail of the power take-off (PTO) for the design process than a simple efficiency map.

The adapted OVT (OVT-E) has been demonstrated in a simulation environment using the WEC-Sim simulation package, and has been shown to be more effective in converting electrical energy than typical

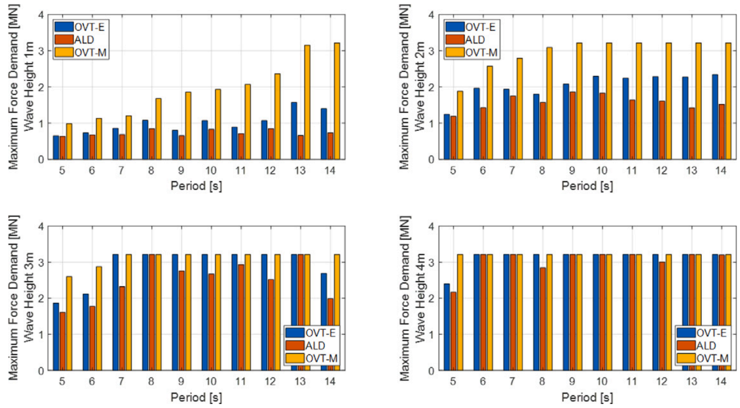

Fig. 23. Max PTO Force — Irregular Wave Simulations (Selected Examples).

OVT for mechanical energy capture and Adaptive Linear Damping (ALD) control, for an example WEC and PTO combination. This result was demonstrated in both regular and irregular wave conditions.

The design method for OVT-E could be adapted to design other controller implementations and could also be utilised by machine learning methods to co-design wave energy power take-off and WEC devices.

The main limitations of the work (one example WEC and PTO system and a more complex simulation environment) are areas to be addressed in future work.

CRediT authorship contribution statement

Adam Stock: Writing – review & editing, Writing – original draft, Visualization, Validation, Supervision, Software, Resources, Project administration, Methodology, Investigation, Funding acquisition, Formal analysis, Data curation, Conceptualization.

Declaration of competing interest

The author declares the following financial interests/personal relationships which may be considered as potential competing interests: Adam Stock reports financial support was provided by Engineering and Physical Sciences Research Council.

Acknowledgements

The author would like to acknowledge the support of the HAPiWEC project team throughout this work. The work was funded by the Engineering and Physical Sciences Research Council (EPSRC), part of United Kingdom Research and Innovation (UKRI) via grant number EP/V040987/1.

References

Ahamed, R., McKee, K., Howard, I., 2020. Advancements of wave energy converters based on power take off (PTO) systems: A review. Ocean Eng. 204, 107248.

Bacelli, G., Genest, R., Ringwood, J.V., 2015. Nonlinear control of flap-type wave energy converter with a non-ideal power take-off system. Annu. Rev. Control 40, 116–126.

Coe, R.G., Bacelli, G., Forbush, D., 2021. A practical approach to wave energy modeling and control. Renew. Sustain. Energy Rev. 142, 110791.

Falnes, J., Kurniawan, A., 2020. Ocean Waves and Oscillating Systems: Linear Interactions Including Wave-Energy Extraction, vol. 8, Cambridge University Press.

Fusco, F., Ringwood, J.V., 2012. A simple and effective real-time controller for wave energy converters. IEEE Trans Sustain Energy 4 (1), 21–30.

García-Violini, D., Peña-Sanchez, Y., Faedo, N., Ringwood, J.V., 2020. An energy-maximising linear time invariant controller (LiTe-Con) for wave energy devices. IEEE Trans. Sustain. Energy 11 (4), 2713–2721.

Hals, J., Falnes, J., Moan, T., 2011. Constrained optimal control of a heaving buoy wave-energy converter. J. Offshore Mech. Arct. Eng. 133 (1).

Hillis, A., Whitlam, C., Brask, A., Chapman, J., Plummer, A., 2020. Active control for multi-degree-of-freedom wave energy converters with load limiting. Renew. Energy 159, 1177–1187.

Keester, A., Leon, J., Tom, N., Ruehl, K., Ogden, D., Forbush, D., Grasberger, J., Husain, S., Topper, M., 2022. Recent Developments in the WEC-Sim Open-Source Design Tool. National Renewable Energy Lab.(NREL), Golden, CO (United States).

Ogden, D., Ruehl, K., Yu, Y.-H., Keester, A., Forbush, D., Leon, J., Tom, N., 2022. Review of WEC-sim development and applications. Int. Mar. Energy J. 5 (NREL/JA-5700-83366).

Penalba, M., Ringwood, J.V., 2019. A high-fidelity wave-to-wire model for wave energy converters. Renew. Energy 134, 367–378.

Pennock, S., Coles, D., Angeloudis, A., Bhattacharya, S., Jeffrey, H., 2022a. Temporal complementarity of marine renewables with wind and solar generation: implications for GB system benefits. Appl. Energy 319, 119276.

Pennock, S., Garcia-Teruel, A., Noble, D.R., Roberts, O., de Andres, A., Cochrane, C., Jeffrey, H., 2022b. Deriving current cost requirements from future targets: Case studies for emerging offshore renewable energy technologies. Energies 15 (5), 1732.

Sergiienko, N., Cazzolato, B., Arjomandi, M., Ding, B., da Silva, L., 2019. Considerations on the control design for a three-tether wave energy converter. Ocean Eng. 183, 469–477.

Sergiienko, N., Cazzolato, B., Hardy, P., Arjomandi, M., Ding, B., 2017. Internal-model-based velocity tracking control of a submerged three-tether wave energy converter. In: Proceedings of the Twelfth European Wave and Tidal Energy Conference. Cork, Ireland.

Stock, A., Gonzalez, C., 2020. Design of optimal velocity tracking controllers for one and two-body point absorber wave energy converters. Renew. Energy 162, 1563–1575.

Stock, A., Gonzalez, C., Robb, D., 2018. Integrated Marine Point Absorber Control Tool Final Stage 2 Project Report. Tech. Rep., Wave Energy Scotland, SgurrControl Ltd..

Stock, A., Gonzalez, C., Robb, D., 2019. IMPACT Toolbox open source code. Wave Energy Scotland Knowledge Library.

Stock, A., Tom, N., Gonzalez, C., 2020. Adapting optimal velocity tracking control to account for WEC constraints and power-take-off efficiencies. IFAC-PapersOnLine 53 (2), 12340–12345.

Trident Energy, 2014. PowerPod Technical Datasheet. Tech. Rep., Trident Energy, pp. 1–3.

Valério, D., Ortigueira, M.D., Sá da Costa, J., 2008. Identifying a transfer function from a frequency response. J. Comput. Nonlinear Dyn. 3 (2), 021207.